mathematics

MDPI

Article

Nonlinear Transient Dynamics of Graphene Nanoplatelets Reinforced Pipes Conveying Fluid under Blast Loads and Thermal Environment

Siyu Liu [1], Aiwen Wang [1,*], Wei Li [1], Hongyan Chen [2], Yufen Xie [1] and Dongmei Wang [3]

[1] School of Applied Science, Beijing Information Science and Technology University, Beijing 100192, China; amalyok922@126.com (S.L.); webbli@163.com (W.L.); yufenxie@163.com (Y.X.)
[2] School of Mechanical Engineering, University of Science and Technology Beijing, Beijing 100083, China; hongyan_chen1028@163.com
[3] College of Electronic Information and Automation, Tianjin University of Science & Techonlogy, Tianjin 300222, China; mutouwang@yeah.net
* Correspondence: wangaiwen@bistu.edu.cn

Abstract: This work aims at investigating the nonlinear transient response of fluid-conveying pipes made of graphene nanoplatelet (GPL)-reinforced composite (GPLRC) under blast loads and in a thermal environment. A modified Halpin–Tsai model is used to approximate the effective Young's modulus of the GPLRC pipes conveying fluid; the mass density and Poisson's ratio are determined by using the Voigt model. A slender Euler–Bernoulli beam is considered for modeling the pipes conveying fluid. The vibration control equation of the GPLRC pipes conveying fluid under blast loads is obtained by using Hamilton's principle. A set of second-order ordinary differential equations are obtained by using the second-order Galerkin discrete method and are solved by using the adaptive Runge–Kutta method. Numerical experiments show that GPL distribution and temperature; GPL weight fraction; pipe length-to-thickness ratio; flow velocity; and blast load parameters have important effects on the nonlinear transient response of the GPLRC pipes conveying fluid. The numerical results also show that due to the fluid–structure interaction, the vibration amplitudes of the GPLRC pipes conveying fluid decay after the impact of blast loads.

Keywords: GPL-reinforced composite; pipes conveying fluid; nonlinear transient dynamics; blast loads; thermal environment

MSC: 74H45

Citation: Liu, S.; Wang, A.; Li, W.; Chen, H.; Xie, Y.; Wang, D. Nonlinear Transient Dynamics of Graphene Nanoplatelets Reinforced Pipes Conveying Fluid under Blast Loads and Thermal Environment. *Mathematics* **2022**, *10*, 2349. https://doi.org/10.3390/math10132349

Academic Editor: Andrey Jivkov

Received: 21 May 2022
Accepted: 1 July 2022
Published: 5 July 2022

1. Introduction

As the main structure for oil and gas transportation, fluid-conveying pipes are widely used in aerospace engineering, marine engineering, water conservancy systems, oil and gas transportation systems, and the petroleum energy/chemical/nuclear industries [1–5]. The structure of pipes employed in engineering nuclear power plants are inevitably impacted by nuclear and fuel explosions [6]. Therefore, in order to improve the explosion resistance of fluid-conveying pipes and to minimize the possibility of catastrophic losses, it is necessary to carry out detailed analyses of the nonlinear transient dynamic behaviors of pipes conveying fluid under blast loads.

In recent years, numerous scholars have paid attention to the study of the mechanical behavior of fluid-conveying pipes. Païdoussis and Gregory did some pioneering work [7]. The transverse vibration equation of horizontal cantilever pipes conveying fluid was derived by using the classical Newton's second law. The complex frequencies of the first four modes of the system were calculated and verified by experiments [8]. In addition, they also studied the vibration instability of fluid-conveying pipes under various boundary conditions [9]. Based on Païdoussis's work, Semler and Li used an energy method and

Newton method to derive the nonlinear governing equations of cantilever pipes conveying fluid and the pipes conveying fluid supported at both ends, respectively [10]. Up to now, these two dynamic equations have been the most widely used. With the development of research on fluid-conveying pipes, structural and mechanical behavior analyses of pipes conveying fluid have been the meaningful topics in the current research. For example, at the beginning of the 21st century, Lee and Chung deduced a new type of nonlinear coupled motion equation of simply supported pipes with two ends [11], based on the Euler–Bernoulli beam theory and the nonlinear Lagrange strain theory. On the basis of the above research, Wang's research team analyzed the vibration frequencies of elastic axial functionally gradient cantilever pipes [12], micro/nanopipes [13,14], flexible bending pipes [15], and cantilever carbon nanotube pipes [16], and discussed the sensitivity of flow rate to the mechanical behavior of pipes conveying fluid. In addition, they conducted a host of work on the vibration of [17] cantilever pipes conveying fluid under nonlinear elastic boundary. Meanwhile, some scholars have paid attention to the mechanical behavior of high-speed pipes conveying fluid. Tan discussed the parametric resonance of the Timoshenko pipeline with pulsating high-speed fluids [18] and super-harmonic resonance [19]. Ye [20] studied the natural frequencies of curved pipes conveying fluid at supercritical fluid. Zhen [21] analyzed the nonlinear vibrations of functionally graded material pipes conveying fluid with initial curvature under supercritical fluid. Ding [22] studied the nonlinear frequency and forced motion of high-speed pipes conveying fluid. Moreover, regarding mechanical analyses, Selmi [23] explored the post-buckling vibration of functionally graded pipes conveying fluid; Khodabakhsh [24] studied nonlinear vibrations and conducted a buckling analysis of Timoshenko pipes conveying fluid; El-Sayed [25] investigated free vibrations through a stability analysis of multi-span pipes conveying fluid; Askarian [26] performed a stability analysis of viscoelastic pipes conveying fluid with different boundary conditions.

With the development of new composite materials, researchers have begun to pay attention to the mechanical behaviors of composite pipes conveying fluid. For example, Amini [27] and Dehrouyeh-Semnani [28] discussed the stability and the thermal resonance response of functionally graded material (FGM) fluid-conveying pipes. Liang conducted a series of studies on the mechanical behaviors of spinning FGM fluid-conveying pipes considering variable velocity [29,30] and multi-span cases [31]. Dang [32] investigated the nonlinear vibrations and stability of FGM fluid-conveying nanotubes. Ghasemi [33] conducted a buckling analysis of multi-walled carbon nanotubes.

Sedighi [34,35] examined the divergence and flutter instabilities of a hetero-nanotube as well as the vibrational characteristics and critical divergence velocity of a hybrid-nanotube constructed using carbon (C) and boron nitride (BN) nanotubes in a magnetic and thermal environment.

GPLs have the advantages of low cost, high Young's modulus, and large contact interface [36]. As a reinforcing material, they are uniformly or gradient distributed in a matrix, which can significantly improve the mechanical and electrical properties of composite materials [37]. Research on the mechanical behavior of GPLRC structures is a hot issue at home and abroad. So far, a large number of studies have focused on the mechanical behaviors of GPLRC beams [38], plates [39,40], shells [6], and joined shells [41]. However, to the best of our knowledge, there are few studies in the literature on mechanical analyses of GPLRC pipes conveying fluid, in particular, for the case of the nonlinear transient dynamic response.

In this paper, the nonlinear transient dynamic response of GPLRC pipes conveying fluid under blast loads is studied, taking into account the thermal environment. The Young's modulus of the GPLRC pipes conveying fluid is estimated using a modified Halpin–Tsai model. The model is established by using Hamilton's principle and solved using the Runge–Kutta method. The effects of the GPLs' content and distribution and geometric parameters, on the nonlinear transient response of the GPLRC pipes conveying fluid, are discussed by numerical simulation.

2. Equations of Motion

A GPLRC pipe conveying fluid as a pinned-pinned supported beam subjected to a blast load was considered. The geometric diagram of the structure with length L, inner radius r_i, and outer radius r_o is depicted in Figure 1. Three GPL distributions, denoted as GPL-U, GPL-O, and GPL-X, are shown in Figure 2. GPL-U represents a uniform distribution of GPLs; GPL-O represents a distribution of GPLs rich in the mid-plane vicinity; GPL-X represents a distribution of GPLs rich in the inner and outer layers. The latter two types also represent FG distributions of GPLs in the thickness direction of the fluid-conveying pipes, in which dark colors represent a greater number of GPLs within that layer.

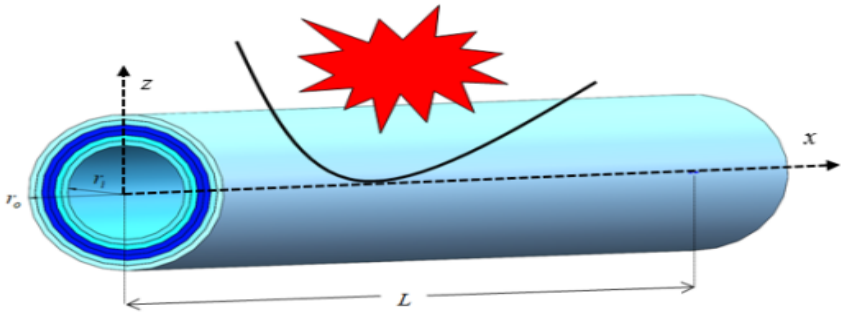

Figure 1. GPLRC fluid-conveying pipe.

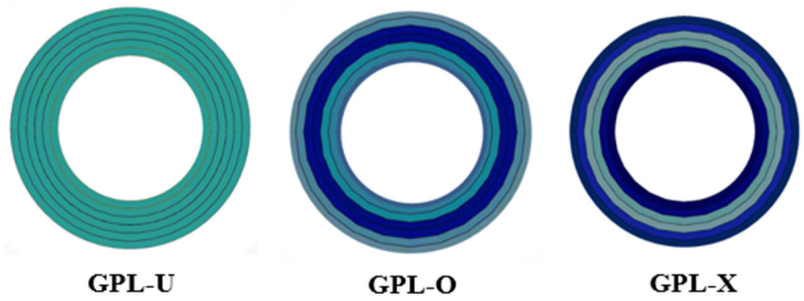

Figure 2. Three radial distribution types of GPLs.

The effective material parameters of the GPLRC pipes conveying fluid, such as Poisson ratio ν_c and Young's modulus E_c, should be clearly introduced, and can be referred to in Appendix A. The nonlinear in-plane strain–displacement relations on the basis of the Von Karman's assumption for the moderately large oscillations of the fluid-conveying pipes can be written as:

$$\varepsilon_{xx} = u'_1 + \frac{1}{2}(u'_3)^2. \tag{1}$$

in which ε_{xx} is the longitudinal strain; u_1 and u_3 are the longitudinal and lateral components of displacement field, respectively. The prime indicates the derivative with respect to coordinate x. On the basis of the Euler–Bernoulli beam model assumption of pipes conveying fluid, the in-plane components of displacement field can be obtained as follows:

$$u_1 = u - zw', u_3 = w. \tag{2}$$

where u and w represent the displacement of the middle surface along the x-axis and z-axis, respectively. Therefore, the longitudinal strain as a function of the longitudinal and transverse displacements of the intermediate plane and the coordinates can be expressed as:

$$\varepsilon_{xx} = u' + \frac{1}{2}(w')^2 - zw'. \tag{3}$$

The temperature variation of the pipes conveying fluid is expressed by ΔT. Therefore, the generalized Hooke's law can be expressed in the following form [28]:

$$\sigma_{xx} = E_c(r)(\varepsilon_{xx} - \varepsilon_T) = E_c(r)\left[u' + \frac{1}{2}(w')^2 - zw' - \alpha(r)\Delta T\right]. \tag{4}$$

Here, σ_{xx} is the stress in the x direction. The thermal stress is expressed as $\varepsilon_T = \alpha(r)\Delta T$, $\alpha(r)$ is the coefficient of thermal expansion.

Through calculation, the potential energy of the fluid-conveying pipes is obtained as:

$$U = \int_V \sigma_{xx}(\varepsilon_{xx} - \varepsilon_T)dV. \tag{5}$$

Substituting Equations (3) and (4) into Equation (5) as the potential energy of the fluid-conveying pipes leads to the following expression:

$$U = \frac{1}{2}\int_0^L \left\{ A_{11}\left[u' + \frac{1}{2}(w')^2\right]^2 + D_{11}(w'')^2 - 2N^T\left[u' + \frac{1}{2}(w')^2\right] + N_0^T \right\} dx. \tag{6}$$

In which

$$A_{11} = \sum_{i=1}^{N_L}\int_0^{2\pi}\int_{r_i}^{r_{i+1}} E_c(r)rdrd\theta. \tag{7}$$

$$D_{11} = \sum_{i=1}^{N_L}\int_0^{2\pi}\int_{r_i}^{r_{i+1}} E_c(r)r^2\sin^2(\theta)rdrd\theta. \tag{8}$$

$$N^T = \sum_{i=1}^{N_L}\int_0^{2\pi}\int_{r_i}^{r_{i+1}} E_c(r)\alpha_c(r)\Delta Trdrd\theta. \tag{9}$$

$$N_0^T = \sum_{i=1}^{N_L}\int_0^{2\pi}\int_{r_i}^{r_{i+1}} E(r)c(\alpha_c(r)\Delta T)^2rdrd\theta. \tag{10}$$

where A_{11} and D_{11} are the extensional and the bending stiffness coefficients, respectively; N^T and N_0^T are the thermal stress resultants. It is worth noting that the thermal moment is zero due to symmetrical distribution of the material with respect to the neutral axis of the pipes conveying fluid.

The kinetic energy of the GPLRC pipes conveying fluid can be expressed as:

$$T_p = \frac{1}{2}m\int_0^L \left[(\dot{w})^2 + (\dot{u})^2\right]dx. \tag{11}$$

In addition, the kinetic energy of fluid can be written as follows:

$$T_f = \frac{1}{2}M\int_0^L \left[\left(\dot{u} + V\left(1 + u'\right)\right)^2 + \left(\dot{w} + Vw'\right)^2\right]dx. \tag{12}$$

The expression of virtual work caused by fluid lateral motion and viscous damping produced by the GPLRC pipes conveying fluid is:

$$\delta W_D = -\int_0^L c_w\frac{\partial w}{\partial t}\delta w dx. \tag{13}$$

when the GPLRC pipes conveying fluid is impacted by blast load, the virtual work is calculated as follows:

$$\delta W_P = \int_0^L p\delta w dx. \tag{14}$$

In Equations (11)–(14), m, M, c_w, p, V are the mass per unit of the GPLRC pipe, the mass per unit of fluid, viscosity coefficient, explosion pressure, and fluid velocity, respectively. The non-linear governing equations of the GPLRC pipes conveying fluid under blast load can be obtained by using Hamilton's principle:

$$\delta\int_{t_1}^{t_2}\Big(T_p+T_f-U\Big)dt+\int_{t_1}^{t_2}(\delta W_D+\delta W_P)dt=0. \tag{15}$$

Substitution of Equations (6), (11), and (12) into Equation (15) results in the following nonlinearly coupled partial differential equations of motion in the longitudinal and the lateral directions respectively:

$$\begin{aligned}&\delta u:-\Big(A_{11}\Big[u'+\tfrac{1}{2}w'^2\Big]\Big)'+MV^2u''+2MV\dot{u}'+(m+M)\ddot{u}=0.\\&\delta w:D_{11}w^{(4)}+\big(MV^2+NT\big)w''-\Big(A_{11}\Big[u'+\tfrac{1}{2}w'^2\Big]w'\Big)'+c_w\dot{w}+2MV\dot{w}'+(M+m)\ddot{w}=p.\end{aligned} \tag{16}$$

Furthermore, the following natural and essential boundary conditions are deduced:

$$\delta u:A_{11}\left(u'+\frac{1}{2}w'^2\right)-MV^2\big(1+u'\big)-2MV\big(1+\dot{u}\big)+N^T=0;u=u_s. \tag{17}$$

$$\delta w:-D_{11}w'''-\Big(MV^2+N^T\Big)w'-2MV\dot{w}+\left(A_{11}\left[u'+\frac{1}{2}w'^2\right]\right)w'=0;w=w_s. \tag{18}$$

$$\delta w\prime:D_{11}w''=0;w'=w'_s. \tag{19}$$

According to [28], the time-dependent terms $(m+M)\ddot{u}$ and $2MV\dot{u}'$ are negligible, and MV^2 is much smaller than A_{11}. Then, we reformulate the longitudinal equation of the governing equation, i.e., Equation (17) as:

$$A_{11}\left(u'+\frac{1}{2}w'^2\right)'=0. \tag{20}$$

The left and right ends of the GPLRC pipes conveying fluid are pinned. Therefore, the longitudinal boundary condition can be expressed as:

$$u(x=0)=u(x=L)=0. \tag{21}$$

Due to Equations (20) and (21), u' can be written as a function of w' as follows:

$$u'=\frac{1}{2}\left(\frac{1}{L}\int_0^L w'^2dx-w'^2\right). \tag{22}$$

Substitution of Equation (22) into Equation (16) as well as Equations (18) and (19) results in the following new governing equation, i.e., Equation (23) and corresponding boundary conditions, i.e., Equations (24) and (25) in terms of the lateral motion, respectively:

$$D_{11}w^{(4)}+\left[MV^2+N-T\frac{A_{11}}{2L}\left(\int_0^L w'^2dx\right)\right]w''+c_w\dot{w}+2MV\dot{w}'+(M+m)\ddot{w}=p. \tag{23}$$

$$-D_{11}w'''-MV^2w'-MV\dot{w}+\frac{A_{11}}{2L}\left(\int_0^L w'^2dx\right)w'=0;w=w_s. \tag{24}$$

$$D_{11}w''=0;w'=w'_s. \tag{25}$$

Assuming that the explosion source has a certain distance from the GPLRC pipes conveying fluid, the impact moment of explosion load can be expressed as the Friedlander equation [6]:

$$p(t)=p_0\big(1-t/t_p\big)e^{\frac{-\gamma t}{t_p}}. \tag{26}$$

In the equation, p_0 is the explosion pressure peak, t_p is the explosion action time, γ is the attenuation parameter, and t represents the time.

According to the obtained nonlinear partial differential equation of transverse motion of the GPLRC pipes conveying fluid, it can be discretized into a set of nonlinear coupled

ordinary differential equations with finite degrees of freedom by using the Galerkin method. In order to obtain the discrete form of the motion control equation, the following series expansion with a set of orthogonal functions is selected:

$$w(x,\tau) = \sum_{n=1}^{N} \psi_n(x) q_n(\tau). \tag{27}$$

where $\psi_n(x) = \sin\left(\frac{n\pi x}{L}\right)$ [42] represents the n-th eigenfunction of the transverse vibration of the GPLRC pipes conveying fluid. In addition, $q_n(\tau)$ represents the n-th generalized coordinate of transverse motion.

The transverse motion equation of the GPLRC pipes conveying fluid is discretized, and a set of nonlinear coupled ordinary differential equations are obtained by using the Galerkin technique [43,44]:

$$M_{ij}\ddot{q}_j + \left(C_{ij}^1 + C_{ij}^2\right)\dot{q}_j + K_{ij}^L q_j + K_{ijkl}^{NL} q_j q_k q_l = F_i, i, j, k, l = 1, 2, \ldots, N \tag{28}$$

in which

$$\begin{array}{l} M_{ij} = (m+M)\int_0^L \psi_i \psi_j dx,\ C_{ij}^1 = C_w \int_0^L \psi_i \psi_j dx,\ C_{ij}^2 = 2mV\int_0^L \psi_i \psi'_j dx. \\ K_{ij}^L = D\int_0^L \psi_i \psi_j^{(4)} dx + \left(MV^2 + N^T\right)\int_0^L \psi_i \psi''_j dx, \\ K_{ijkl}^{NL} = -\frac{A_{11}}{2L}\int_0^L \psi_i \psi''_j dx \int_0^L \psi'_k \psi'_l dx,\ F_i = \int_0^L p\psi_i dx. \end{array} \tag{29}$$

In which, $i = 1, 2, \ldots, N$.

3. Numerical Simulations

In this section, the nonlinear transient dynamic behavior of GPLRC pipes conveying fluid with three distribtuions of GPLs under blast loads is considered. Here, epoxy resin and GPLs are selected as the polymer matrix and reinforcement [45]. Then, the numerical results are obtained by using the adaptive Runge–Kutta method with zero initial value (w_1, w_2) and time step 10^{-8} s. The fluid is taken as lead with the following density $\rho_f = 10,678$ Kg/m^3 and melting point 600.6 K. The reference temperature is considered to be $T_0 = 300$ K. Therefore, the minimum temperature rise at the inner surface of the GPLRC pipes conveying fluid equals $\Delta T_{\min} = 300.6$ K. The following geometric and material property parameters [45] listed in Table 1 remain unchanged, except as specifically stated.

Table 1. Material parameters and geometric parameters of pipes.

Parameters	Data	Parameters	Data
r_i	0.2 m	E_M	3.0 GPa
r_o	0.225 m	v_M	0.34
L	$20{\cdot}r_o$	v_G	0.186
l_G	2.5 μm	f_G	1.2%
w_G	1.5 μm	P_0	10^8 N/m^2
h_G	1.5 nm	t_p	0.25 ms
N_l	10	T_0	300 K
ρ_G	1.06 g/cm^3	T	600.6 K
E_G	1.01 TPa	c_w	0.02
ρ_M	1.2 g/cm^3	V	5 m/s

In order to show the accuracy and precision of the proposed formulation and the solution method, some comparison studies are conducted, as there have been no suitable results on the nonlinear transient response of GPLRC pipes conveying fluid. The first three natural frequencies of the simply supported pipes conveying fluid with the fluid velocities $V = 0$ m/s, 15 m/s, 25 m/s, 35 m/s, 45 m/s, 55 m/s are calculated by using the Galerkin technique and are compared with the open literature. The material and

geometry parameters are illustrated in Table 2. There is good agreement between the results obtained by the present study and those by Xu [42] and by Housner [46] as well as the FEM results using software Ansys in Table 3, which demonstrates the reliability of the model and methods employed in this paper. In addition, the same accuracy of fundamental frequencies with the degrees of freedom N = 2, 4, and 6 in Equation (27) (shown in Figure 3) implies that N = 2 can be taken for the next whole simulation.

Table 2. Material and geometry parameters used in studies by Xu [42] and Housner [46].

Parameters	Data	Parameters	Data
Elasticity modulus	310 Gpa	Density of the pipe	8200 kg/m^3
r_i	0.186 m	Density of the fluid	908.2 kg/m^3
r_o	0.162 m	Pipe length	32 m

Table 3. Comparisons between the FEM results and theoretical values.

Flow Velocity (m/s)	Reference	0	15	25	35	45	55
1st mode	Present	4.3732	4.2872	4.1306	3.8863	3.5390	3.0593
	FEM	4.3732	4.2870	4.1293	3.8807	3.5222	3.0145
	Xu [42]	4.3732	4.2921	4.1441	3.9116	3.5781	3.1115
	Housner [46]	4.3732	4.2971	4.1576	3.9372	3.6183	3.1660
2nd mode	Present	17.4928	17.4174	17.2827	17.0793	16.8051	16.4573
	FEM	17.4928	17.4123	17.2682	17.0499	16.7544	16.3775
	Xu [42]	17.4928	17.4171	17.2816	17.0765	16.7991	16.4457
	Housner [46]	17.4928	17.3922	17.2122	16.9390	16.5686	16.0855
3rd mode	Present	39.3587	39.2865	39.1580	38.9648	38.7063	38.3819
	FEM	39.3587	39.2783	39.1350	38.9190	38.6292	38.2638
	Xu [42]	39.3587	39.2858	39.1559	38.9602	38.6978	38.3672
	Housner [46]	-	-	-	-	-	-

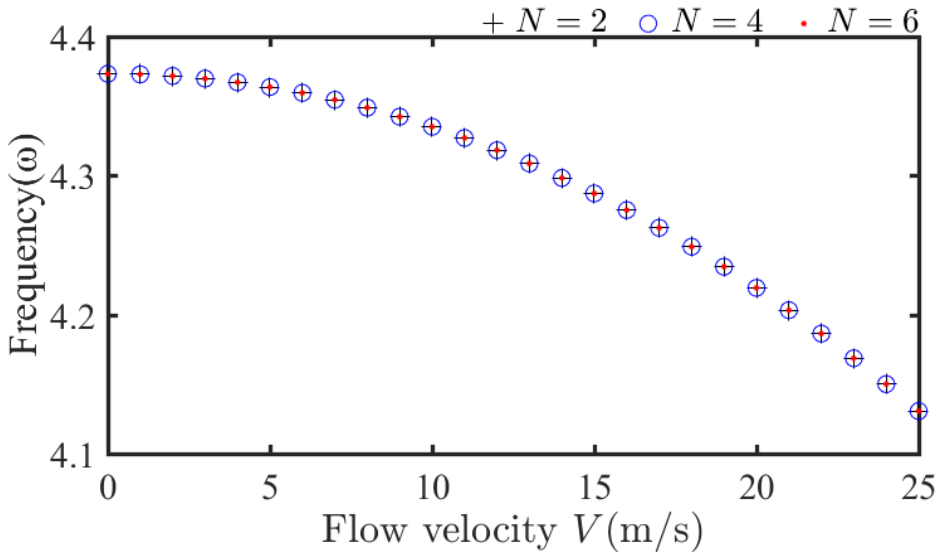

Figure 3. The fundamental variation frequency of pipes conveying fluid frequency versus flow velocity.

As shown in Figure 4, the vibrations of GPLRC pipes conveying fluid with a uniform distribution of GPLs under the impact of blast load will lead to energy loss over time and the amplitude of the vibrations will have an obvious downward trend.

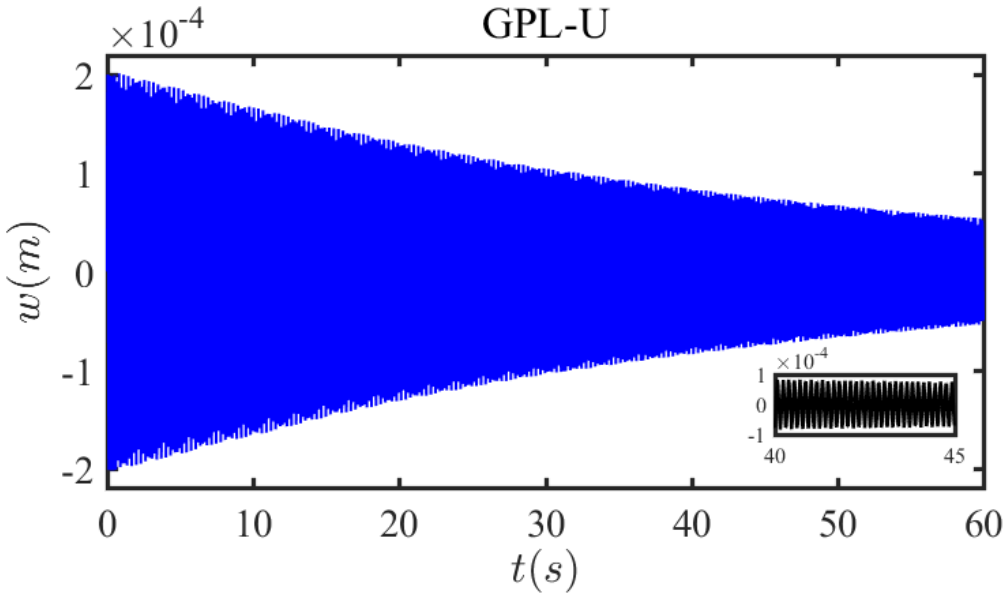

Figure 4. Time history diagram of GPLRC pipes conveying fluid with a uniform disribuiton of GPLs.

Figure 5 indicates a higher frequency and lower amplitude of vibrations, because the structural stiffness is increased by the addition of GPLs. However, the amplitude difference of the GPLRC pipes conveying fluid under three distribution modes is not significant. This is because the pipes conveying fluid are slender hollow beam structures with thin thickness. The results imply that in an actual industrial production process, any GPL distribution can be selected for structure production according to convenience. In the follow-up study, the GPL-X distribution is selected for research and discussion.

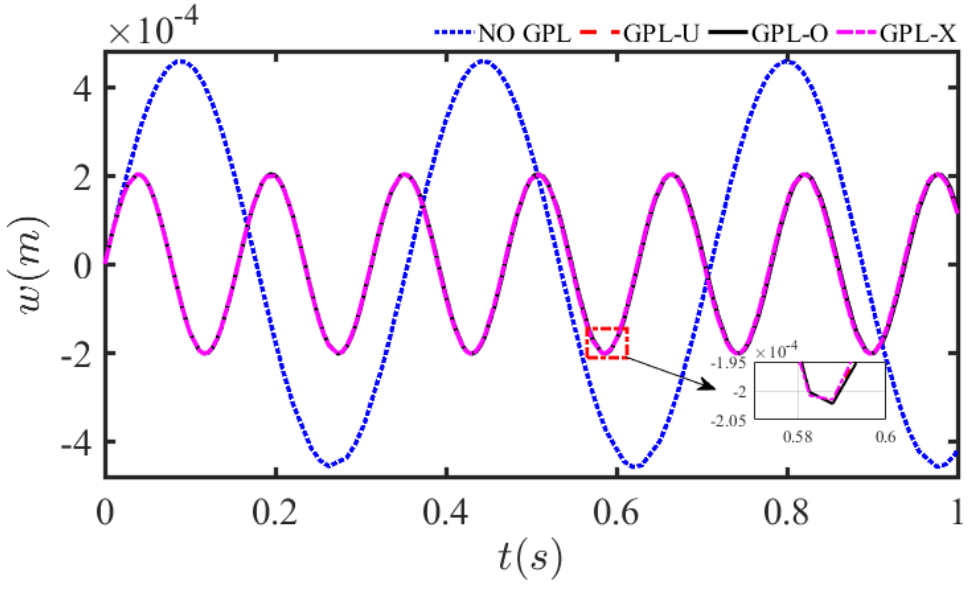

Figure 5. Effect of GPL distributions on the nonlinear transient vibrations of fluid-conveying pipes.

The parameters of blast load are one of the most important factors in an analysis of nonlinear transient dynamics. Given $\Delta T = 300.6$ K, Figures 6–8, respectively, introduce the influence of decay parameter ($\gamma = 0.1, 1, 2$), explosion duration ($t_p = 0.25$ ms, 0.3 ms, 0.4 ms), and explosion pressure index ($p = 10^4$ N/m^2, 10^5 N/m^2, 10^6 N/m^2) on the effects of nonlinear transient dynamic behavior of GPLRC pipes conveying fluid. As can be seen from Figure 6, the vibration amplitude of the pipes conveying fluid decreases as the attenuation parameter increases from 0.1 to 2, due to the gradually attenuated blast load. Furthermore,

according to Figures 7 and 8, it can be inferred that the vibration amplitude is increased, whether or not the explosion duration is longer or the peak explosion pressure is greater. However, the transient blast load has little effect on vibration frequency, mainly because the time it acts on the structure is too short. In the following analysis, the blast load parameter ($\gamma = 0.1, t_p = 0.25$ ms, $p = 10^5$ N/m^2) selection remains unchanged.

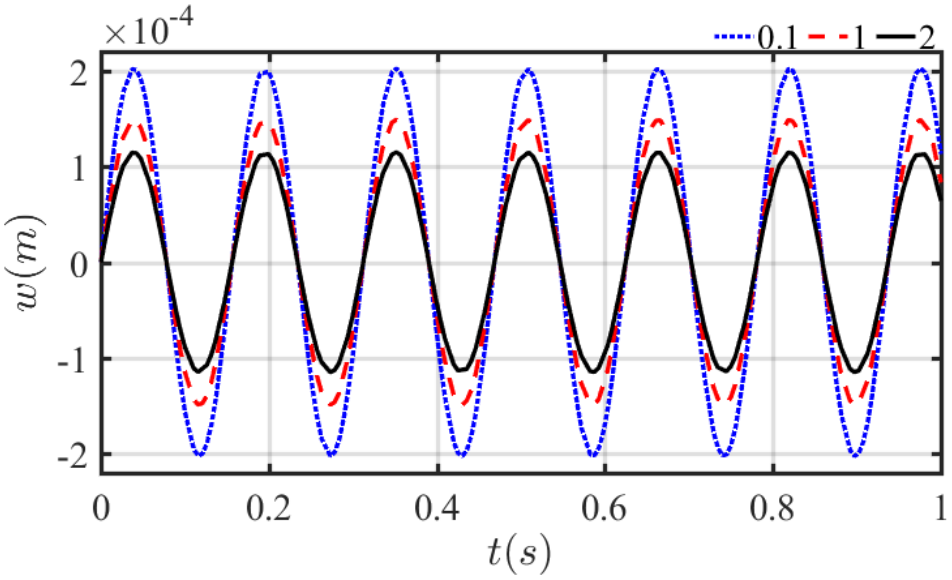

Figure 6. Effect of decay parameters γ on pipes conveying fluid nonlinear transient vibration.

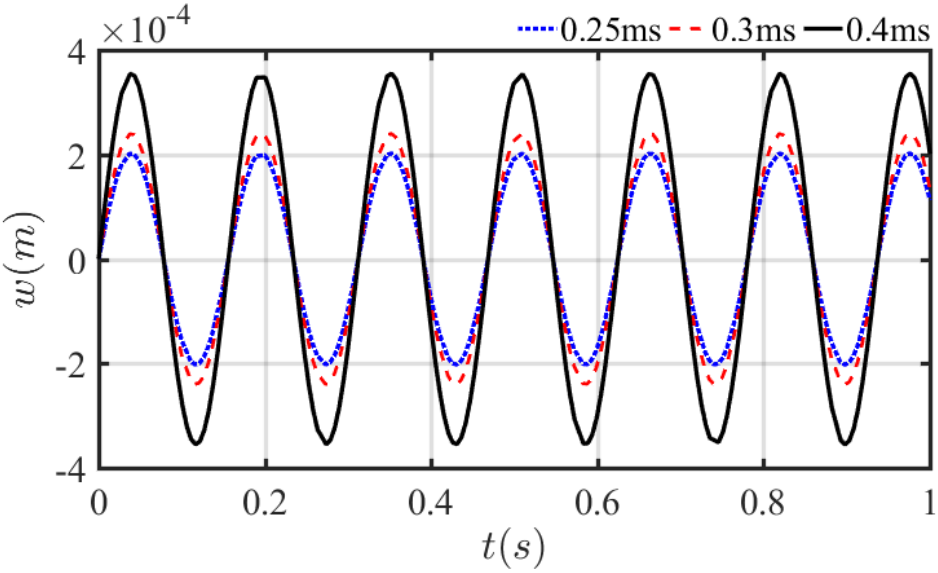

Figure 7. Effect of explosion time t_p on pipes conveying fluid nonlinear transient vibration.

Considering the above temperature difference $\Delta T = 300.6$ K as the basic temperature change unit, we investigated the influence of temperature differences $\Delta T, 2\Delta T, 4\Delta T$ on vibrations in GPLRC pipes conveying fluid. It can be seen from Figure 9 that the vibration amplitude becomes larger and the vibration frequency of the structure becomes smaller with an increase in temperature difference. This is due to the lower elastic modulus with the higher temperature.

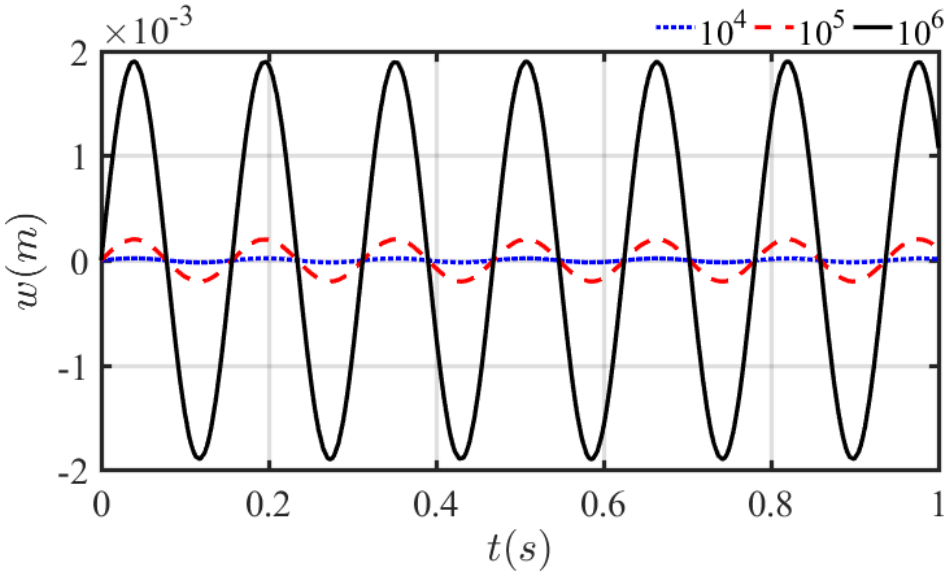

Figure 8. Effect of pressure peak index p on pipes conveying fluid nonlinear transient vibration.

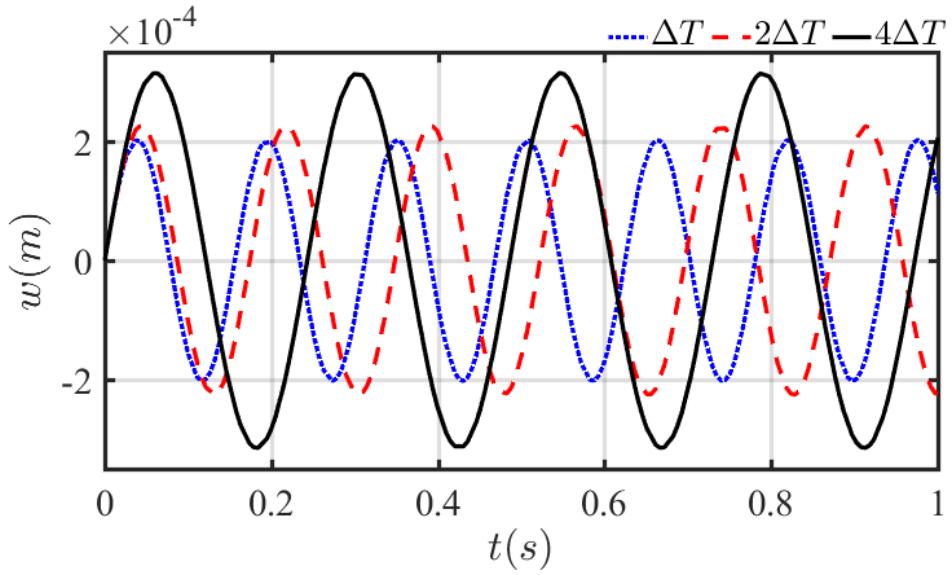

Figure 9. Effect of temperature differences on pipes conveying fluid nonlinear transient vibration.

Figure 10 displays the vibration time history of GPLRC pipes conveying fluid under different GPLs mass fractions. The vibration frequency of the pipes conveying fluid increases and the amplitude decreases with a change in GPL mass fraction from 0 to 1.2%. This is because the addition of GPLs improves the system's stiffness and also enhances the GPL impact resistance of the pipes conveying fluid.

Figure 11 shows the effect of the GPL length-to-thickness ratio with a constant GPL thickness. The higher the ratio, the faster the vibration frequency because of the larger contact area between the pipe and GPLs, which effectively increases the stiffness of the structure.

Figure 12 shows the time history diagram of the vibrations of the GPLRC pipes conveying fluid at different flow rates. It can be observed that an increase in the flow rate $V = (0\ \mathrm{m/s}, 5\ \mathrm{m/s}, 20\ \mathrm{m/s}, 50\ \mathrm{m/s})$ causes a reduction in the vibration frequency of the GPLRC pipes conveying fluid and an increment of vibration amplitude, which can be seen by taking 10–11 s as an example. The main reason is that the increasing fluid velocity can weaken the pipe stiffness.

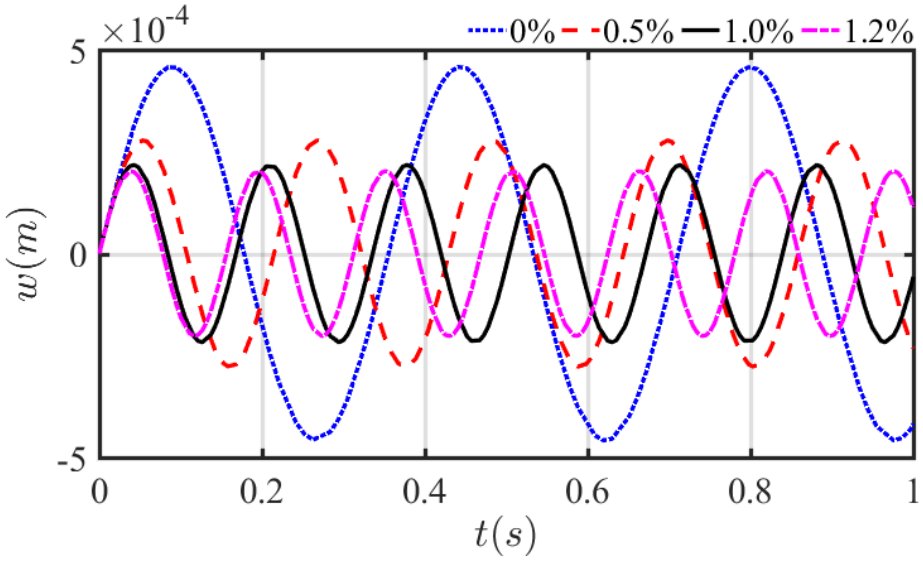

Figure 10. Effect of GPL mass fraction on pipes conveying fluid nonlinear transient vibration.

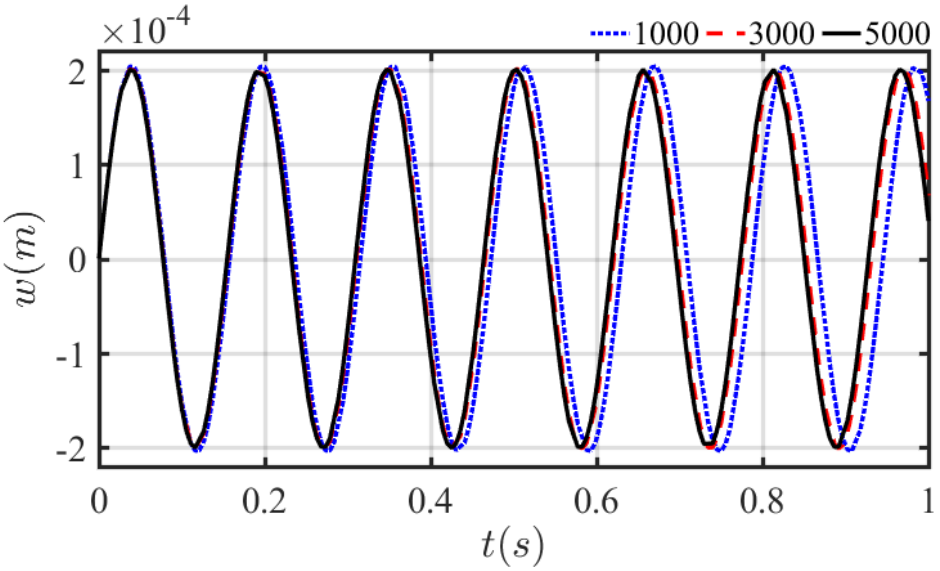

Figure 11. Effects of the GPL length-to-thickness ratio on the GPLRC pipes conveying fluid nonlinear transient vibration.

Here, we give the inner and outer diameters $r_i = 0.20$ m and $r_0 = 0.225$ m of the GPLRC pipes conveying fluid as a constant, and study the effect of the structure's length-to-thickness ratio on its nonlinear transient vibration. As shown in Figure 13, there is an obvious increase in the maximum amplitude of the structure with an increase in the length-to-thickness ratio; the inverse results are obtained for the vibration frequency. This phenomenon indicates that under certain thicknesses within the acceptable accuracy range, appropriately increasing the length-to-thickness ratio of the pipes conveying fluid is more helpful for reducing the vibration frequency of the pipes conveying fluid in the actual production process.

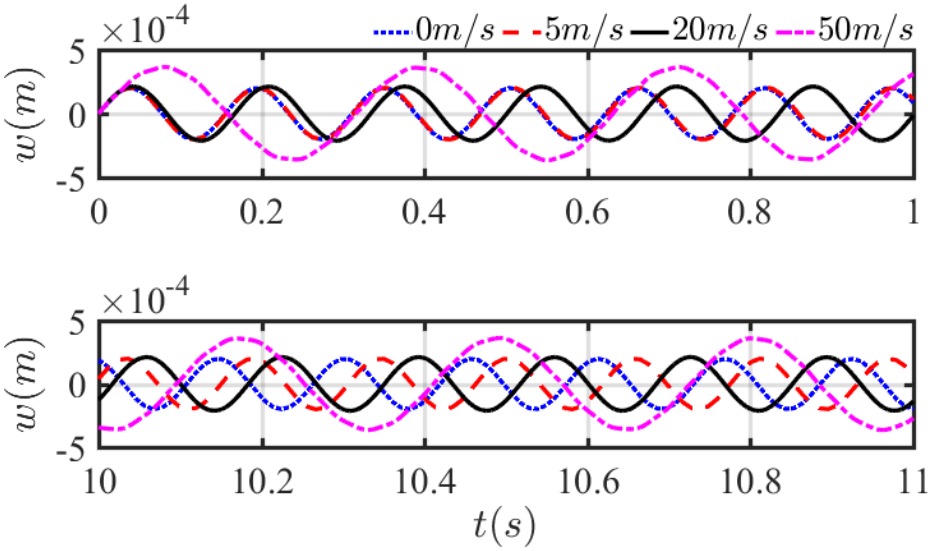

Figure 12. Effects of flow rates on the nonlinear transient vibration of GPLRC pipes conveying fluid.

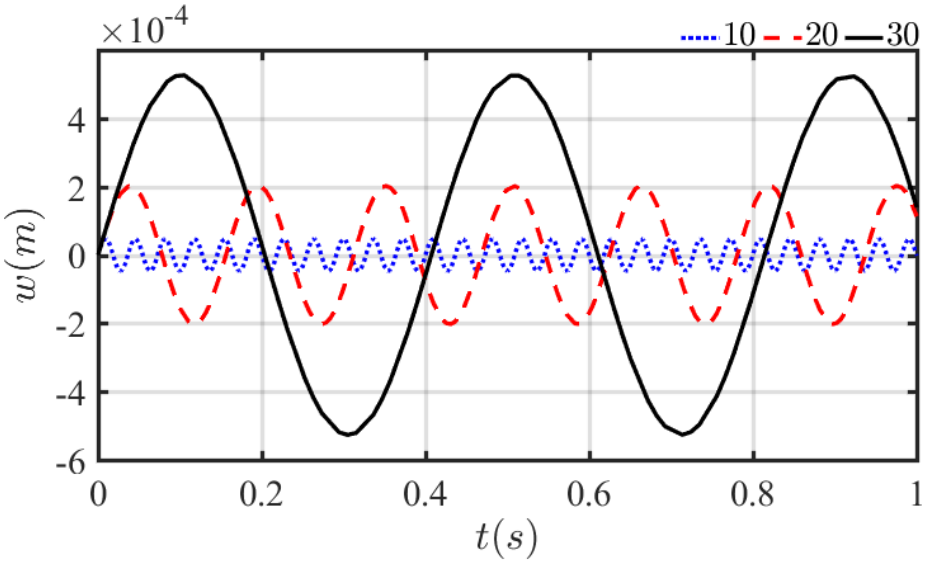

Figure 13. Effects of pipes conveying fluid length-to-thickness ratio on nonlinear transient vibrations.

4. Conclusions and Discussions

In the framework of this study, nonlinear transient dynamic responses of GPLRC pipes conveying fluid subjected to time-varying blast loads were analyzed by using the Galerkin method in conjunction with the adaptive Runge–Kutta method. The polymer matrix and reinforcement were considered to be epoxy resin and GPLs, respectively, and the fluid was regarded to be lead. According to Hamilton's principle, nonlinear partial differential governing equations of pipes conveying fluid were derived. The numerical simulations mainly focused on analyzing the effects of GPL content, fluid velocity, geometry size, and blast load parameters on the vibration frequencies and vibration amplitudes of GPLRC pipes conveying fluid. The accuracy of the model was confirmed by comparing the frequencies with the published results in the literature. Based on the parametric study, the following important conclusions are presented:

- GPLs as reinforcement can enhance the vibration frequency and impact resistance of pipes conveying fluid, but their distribution mode has little effect. This also means that in an industrial production process, the most convenient and economical GPL distribution among the three distribution modes can be selected for production.

- Transient load parameters have significant influence on vibration amplitude and little influence on vibration frequency.
- Vibration frequency has a descending trend with respect to temperature difference, pipes conveying fluid length-to-thickness ratios, and flow rates; however, the opposite conclusion was obtained for the effects of GPL length-to-thickness ratio and vibration amplitude.

Author Contributions: Conceptualization, S.L. and A.W.; methodology, S.L.; software, S.L. and W.L.; validation, S.L., W.L. and H.C.; formal analysis, S.L. and Y.X.; investigation, S.L. and A.W.; writing—original draft preparation, S.L. and A.W.; writing—review and editing, S.L. and D.W.; supervision, A.W.; funding acquisition, A.W. and H.C. All authors have read and agreed to the published version of the manuscript.

Funding: This research was funded by the National Natural Science Foundation of China (11772063, 11832003, 11902038 and 11732005) and the Guangdong Basic and Applied Basic Research Foundation (2021A1515110945).

Institutional Review Board Statement: Not applicable.

Informed Consent Statement: Not applicable.

Data Availability Statement: Not applicable.

Acknowledgments: The authors sincerely thank the anonymous reviewers for their valuable comments that have led to the present improved version of the original manuscript.

Conflicts of Interest: The authors declare no conflict of interest.

Appendix A

A model of pipes conveying fluid with total distribution layers N_L is considered. The Young's modulus of each layer can be calculated by using a modified Halpin–Tsai model [38,40]. The results are as follows:

$$E_c^{(k)} = \frac{3}{8}\frac{1+\xi_L\eta_L V_G^{(k)}}{1-\eta_L V_G^{(k)}} \times E_M + \frac{5}{8}\frac{1+\xi_W\eta_W V_G^{(k)}}{1-\eta_W V_G^{(k)}} \times E_M. \tag{A1}$$

In which,

$$\eta_L = \frac{(E_G/E_M)-1}{(E_G/E_M)+\xi_L};\ \eta_W = \frac{(E_G/E_M)-1}{(E_G/E_M)+\xi_W};\ \xi_L = \frac{2l_G}{h_G};\ \xi_W = \frac{2w_G}{h_G}. \tag{A2}$$

E_M and E_G are Young's moduli of the GPLs and matrix, respectively; l_G, w_G, and h_G are the average length, width, and thickness of the GPLs, respectively. The k-th layer GPL volume fraction is given by:

$$V_G^{(k)} = \frac{f_G^{(k)}}{f_G^{(k)} + (\rho_G/\rho_M)(1-f_G^{(k)})}. \tag{A3}$$

where $f_G^{(k)}$ is GPL weight fraction of the k-th layer for the three GPL distribution patterns of GPLRC pipes conveying fluid, and the distribution patterns 1–3 are as follows:

Pattern 1:

$$f_G^{(k)} = W_G. \tag{A4}$$

Pattern 2:

$$f_G^{(k)} = 4W_G\left(\frac{N_L+1}{2} - \left|k - \frac{N_L+1}{2}\right|\right)/(2+N_L). \tag{A5}$$

Pattern 3:

$$f_G^{(k)} = 4W_G\left(\frac{1}{2} + \left|k - \frac{N_L+1}{2}\right|\right)/(2+N_L). \tag{A6}$$

where, $k = 1, 2, \ldots, N_L$ and W_G is the total GPL weight fraction. The effective material properties $P_c^{(k)}$ of the GPLRC pipes are expressed by following the rule of mixtures [38,40]:

$$P_c^{(k)} = P_G V_G^{(k)} + P_M (1 - V_G^{(k)}) \,. \tag{A7}$$

where the material properties $P_c^{(k)}$ represent mass density $\rho_c^{(k)}$, Poisson's ratio $\nu_c^{(k)}$, and the thermal expansion coefficient $\alpha_c^{(k)}$, respectively. Moreover, the subscripts "G", "M", and "c" represent GPLs, matrix, and nanocomposite, respectively.

References

1. Païdoussis, M.P.; Li, G.X. Pipes conveying fluid: A model dynamical problem. *J. Fluids Struct.* **1993**, *7*, 137–204. [CrossRef]
2. Wang, L.; Dai, H.L. Vibration and enhanced stability properties of fluid-conveying pipes with two symmetric elbows fitted at downstream end. *Arch. Appl. Mech.* **2012**, *82*, 155–161. [CrossRef]
3. Païdoussis, M.P. The canonical problem of the fluid-conveying pipe and radiation of the knowledge gained to other dynamics problems across Applied Mechanics. *J. Sound Vib.* **2008**, *310*, 462–492. [CrossRef]
4. Wang, L. Size-dependent vibration characteristics of fluid-conveying microtubes. *J. Fluids Struct.* **2010**, *26*, 675–684. [CrossRef]
5. Xiaoxu, M.A.; Maocheng, T.; Guanmin, Z.; Xueli, L. Numerical investigation on gas-liquid two-phase flow-induced vibration in a horizontal tube. *Shock Vib.* **2016**, *35*, 204–210. [CrossRef]
6. Wang, A.W.; Chen, H.Y.; Zhang, W. Nonlinear transient response of doubly curved shallow shells reinforced with graphene nanoplatelets subjected to blast loads considering thermal effects. *Compos. Struct.* **2019**, *225*, 111063. [CrossRef]
7. Gregory, R.W.; Païdoussis, M.P. Unstable oscillation of tubular cantilevers conveying fluid I. Theory. *Proc. R. Soc. Lond. Ser. A Math. Phys. Sci.* **1966**, *293*, 512–527.
8. Gregory, R.W.; Païdoussis, M.P. Unstable Oscillation of Tubular Cantilevers Conveying Fluid. II. Experiments. *Proc. R. Soc. Lond. Ser. A Math. Phys. Sci.* **1966**, *293*, 528–542.
9. Païdoussis, M.P.; Issid, N.T. Dynamic stability of pipes conveying fluid. *J. Sound Vib.* **1974**, *33*, 267–294. [CrossRef]
10. Semler, C.; Li, G.X.; Païdoussis, M.P. The non-linear equations of motion of pipes conveying fluid. *J. Sound Vib.* **1994**, *169*, 577–599. [CrossRef]
11. Lee, S.I.; Chung, J. New non-linear modeling for vibration analysis of a straight pipe conveying fluid. *J. Sound Vib.* **2002**, *254*, 313–325. [CrossRef]
12. Zhou, X.W.; Dai, H.L.; Wang, L. Dynamics of axially functionally graded cantilevered pipes conveying fluid. *Compos. Struct.* **2018**, *190*, 112–118. [CrossRef]
13. Guo, Y.; Xie, J.H.; Wang, L. Three-dimensional vibration of cantilevered fluid-conveying micropipes—Types of periodic motions and small-scale effect. *Int. J. Non-Linear Mech.* **2018**, *102*, 112–135. [CrossRef]
14. Dai, H.L.; Wang, L.; Abdelkefi, A.; Ni, Q. On nonlinear behavior and buckling of fluid-transporting nanotubes. *Int. J. Eng. Sci.* **2015**, *87*, 13–22. [CrossRef]
15. Lin, W.; Qiao, N. In-plane vibration analyses of curved pipes conveying fluid using the generalized differential quadrature rule. *Comput. Struct.* **2008**, *86*, 133–139. [CrossRef]
16. Wang, L.; Hong, Y.Z.; Dai, H.L.; Ni, Q. Natural frequency and stability tuning of cantilevered CNTs conveying fluid in magnetic field. *Acta Mech. Solida Sin.* **2016**, *29*, 567–576. [CrossRef]
17. Qian, Q.; Wang, L.; Ni, Q. Nonlinear Responses of a fluid-conveying pipe embedded in nonlinear elastic foundations. *Acta Mech. Solida Sin.* **2008**, *21*, 170–176. [CrossRef]
18. Tan, X.; Ding, H. Parametric resonances of Timoshenko pipes conveying pulsating high-speed fluids. *J. Sound Vib.* **2020**, *485*, 115594. [CrossRef]
19. Tan, X.; Ding, H.; Sun, J.Q.; Chen, L.Q. Primary and super-harmonic resonances of Timoshenko pipes conveying high-speed fluid. *Ocean Eng.* **2020**, *203*, 107258. [CrossRef]
20. Ye, S.Q.; Ding, H.; Wei, S.; Ji, J.C.; Chen, L.Q. Non-trivial equilibriums and natural frequencies of a slightly curved pipe conveying supercritical fluid. *Ocean Eng.* **2021**, *227*, 108899. [CrossRef]
21. Zhen, Y.X.; Gong, Y.F.; Tang, Y. Nonlinear vibration analysis of a supercritical fluid-conveying pipe made of functionally graded material with initial curvature. *Compos. Struct.* **2021**, *268*, 113980. [CrossRef]
22. Tan, X.; Ding, H.; Chen, L.Q. Nonlinear frequencies and forced responses of pipes conveying fluid via a coupled Timoshenko model. *J. Sound Vib.* **2019**, *455*, 241–255. [CrossRef]
23. Selmi, A.; Hassis, H. Vibration analysis of post-buckled fluid-conveying functionally graded pipe. *Compos. Part C* **2021**, *4*, 100117. [CrossRef]
24. Khodabakhsh, R.; Saidi, A.R.; Bahaadini, R. An analytical solution for nonlinear vibration and post-buckling of functionally graded pipes conveying fluid considering the rotary inertia and shear deformation effects. *Appl. Ocean Res.* **2020**, *101*, 102277. [CrossRef]
25. El-Sayed, T.A.; El-Mongy, H.H. Free vibration and stability analysis of a multi-span pipe conveying fluid using exact and variational iteration methods combined with transfer matrix method. *Appl. Math. Model.* **2019**, *71*, 173–193. [CrossRef]

26. Askarian, A.R.; Permoon, M.R.; Zahedi, M.; Shakouri, M. Stability analysis of viscoelastic pipes conveying fluid with different boundary conditions described by fractional Zener model. *Appl. Math. Model.* **2022**, *103*, 750–763. [CrossRef]
27. Amini, Y.; Heshmati, M.; Daneshmand, F. Effects of longitudinal fins on dynamic stability of pipes conveying fluid made of functionally graded material. *Mar. Struct.* **2021**, *79*, 103058. [CrossRef]
28. Dehrouyeh-Semnani, A.M.; Dehdashti, E.; Reza Hairi Yazdi, M.; Nikkhah-Bahrami, M. Nonlinear thermo-resonant behavior of fluid-conveying FG pipes. *Int. J. Eng. Sci.* **2019**, *144*, 103141. [CrossRef]
29. Liang, F.; Gao, A.; Li, X.F.; Zhu, W.D. Nonlinear parametric vibration of spinning pipes conveying fluid with varying spinning speed and flow velocity. *Appl. Math. Model.* **2021**, *95*, 320–338. [CrossRef]
30. Liang, F.; Yang, X.D.; Qian, Y.J.; Zhang, W. Transverse free vibration and stability analysis of spinning pipes conveying fluid. *Int. J. Mech. Sci.* **2018**, *137*, 195–204. [CrossRef]
31. Liang, F.; Gao, A.; Yang, X.D. Dynamical analysis of spinning functionally graded pipes conveying fluid with multiple spans. *Appl. Math. Model.* **2020**, *83*, 454–469. [CrossRef]
32. Dang, V.H.; Sedighi, M.H.; Chan, D.Q.; Civalek, O.; Abouelregal, A.E. Nonlinear vibration and stability of FG nanotubes conveying fluid via nonlocal strain gradient theory. *Struct. Eng. Mech.* **2021**, *78*, 103–116. [CrossRef]
33. Ghasemi, A.; Dardel, M.; Ghasemi, M.H.; Barzegari, M.M. Analytical analysis of buckling and post-buckling of fluid conveying multi-walled carbon nanotubes. *Appl. Math. Model.* **2013**, *37*, 4972–4992. [CrossRef]
34. Sedighi, H.M. Divergence and flutter instability of magneto-thermo-elastic C-BN hetero-nanotubes conveying fluid. *Acta Mech. Sin.* **2020**, *36*, 381–396. [CrossRef]
35. Sedighi, H.M.; Ouakad, H.M.; Dimitri, R.; Tornabene, F. Stress-driven Nonlocal Elasticity for Instability Analysis of Fluid-conveying C-BN Hybrid-nanotube in Magnetic and Thermal Environment. *Phys. Scr.* **2020**, *95*, 065204. [CrossRef]
36. Guo, X.Y.; Zhang, B.; Cao, D.X.; Sun, L. Influence of nonlinear terms on dynamical behavior of graphene reinforced laminated composite plates. *Appl. Math. Model.* **2020**, *78*, 169–184. [CrossRef]
37. Rafiee, M.A.; Rafiee, J.; Wang, Z.; Song, H.H.; Yu, Z.Z.; Koratkar, N. Enhanced mechanical properties of nanocomposites at low graphene content. *ACS Nano* **2009**, *3*, 3884–3890. [CrossRef]
38. Yang, J.; Wu, H.L.; Kitipornchai, S. Buckling and postbuckling of functionally graded multilayer graphene plateletreinforced composite beams. *Compos. Struct.* **2017**, *161*, 111–118. [CrossRef]
39. Guo, H.L.; Cao, S.Q.; Yang, T.Z.; Chen, Y.S. Vibration of laminated composite quadrilateral plates reinforced with graphene nanoplatelets using the element-free IMLS-Ritz method. *Int. J. Mech. Sci.* **2018**, *142–143*, 610–621. [CrossRef]
40. Mao, J.J.; Zhang, W. Linear and nonlinear free and forced vibrations of graphene reinforced piezoelectric composite plate under external voltage excitation. *Compos. Struct.* **2018**, *203*, 551–565. [CrossRef]
41. Chai, Q.D.; Wang, Y.Q. Traveling wave vibration of graphene platelet reinforced porous joined conical-cylindrical shells in a spinning motion. *Eng. Struct.* **2022**, *252*, 113718. [CrossRef]
42. Xu, M.R.; Xu, S.P.; Guo, H.Y. Determination of natural frequencies of fluid-conveying pipes using homotopy perturbation method. *Comput. Math. Appl.* **2010**, *60*, 520–527. [CrossRef]
43. Zhang, W.; Yang, J.; Hao, Y.X. Chaotic vibrations of an orthotropic FGM rectangular plate based on third-order shear deformation theory. *Nonlinear Dyn.* **2010**, *59*, 619–660. [CrossRef]
44. Hao, Y.X.; Zhang, W.; Yang, J. Nonlinear oscillation of a cantilever FGM rectangular plate based on third-order plate theory and asymptotic perturbation method. *Compos. Part B Eng.* **2011**, *42*, 402–413. [CrossRef]
45. Chen, H.Y.; Mao, X.Y.; Ding, H.; Chen, L.Q. Elimination of multimode resonances of composite plate by inertial nonlinear energy sinks. *Mech. Syst. Signal Process.* **2020**, *135*, 106383. [CrossRef]
46. Housner, G.W. Bending Vibrations of a Pipe Line Containing Flowing Fluid. *J. Appl. Mech.* **1952**, *19*, 205–208. [CrossRef]